Available online at www.sciencedirect.com

ScienceDirect

Energy Procedia 77 (2015) 364 – 373

Energy Procedia

5th International Conference on Silicon Photovoltaics, SiliconPV 2015

Outdoor performance of bifacial modules by measurements and modelling

Gaby J.M. Janssen*, Bas B. Van Aken, Anna J. Carr, Agnes A. Mewe

ECN Solar Energy P.O.Box 1, 1755 ZG Petten, the Netherlands

Abstract

We present the outline of a model that calculates the outdoor performance of a bifacial module including optical, electrical and thermal aspects. The *IV* curve for the total module power output is obtained by scaling or weighting the 2-diode parameters of front and rear standard test conditions (STC) module *IV* curves with the calculated front and rear irradiance. Validation and verification of the electrical model are given through simulations and measurements. Annual yield gain predictions based on measured characteristics of bifacial modules are presented and discussed for vertical, east-west bifacial modules relative to south-facing tilted monofacial modules. For a module with a bifaciality factor of 92% in a location like Amsterdam, this predicted annual yield gain is in the order of 10% at albedo 0.2 and 30% at albedo 0.5.

Peer review by the scientific conference committee of SiliconPV 2015 under responsibility of PSE AG

Keywords: Bifacial module, annual energy yield, simulation, SiPV

1. Introduction

Bifacial PV modules and systems have the clear potential to surpass monofacial ones as there are many locations and conditions where the total amount of light on both sides of a module exceeds that of a south-facing (or north-facing in the southern hemisphere) monofacial module with optimum tilt angle. Replacement of a conventional free standing glass-backsheet module by a glass-glass module with bifacial cells can already result in 20% annual energy gain, depending on the albedo [1]. Recent studies by Yusufoglu indicated the energy gain can be further enhanced by

* Corresponding author. Tel.: +31 88 515 4803; fax: +31 88 515 8214
E-mail address: janssen@ecn.nl

Peer review by the scientific conference committee of SiliconPV 2015 under responsibility of PSE AG
doi:10.1016/j.egypro.2015.07.051

optimising the tilt angle and elevation of the module to minimise self-shading and maximise the capture of diffuse light [2]. A special case are vertically mounted modules facing east-west which produce most of their energy in the morning and the afternoon. A recent paper by Gou et al. showed that at locations with a large diffuse fraction of light or a high albedo, like most locations at latitudes > 45° and desert areas, such modules receive more irradiation than conventional monofacial modules oriented versus the equator [1].

The development of solar cells based on n-type silicon substrates favours bifaciality since a metallisation grid can be applied at the rear instead of a full area aluminum back surface field/metallisation. Examples of such cells are the n-Pasha cell [3] developed at ECN (commercialised under the brand name PANDA by Yingli) and the BiSoN cells of ISC Konstanz [4]. Bifacial cells with a p-type substrate are also under development at ECN, as well as at Fraunhofer ISE (BOSCO concept) [5]. The bifacial concept is equally feasible for heterojunction cells, and even back contacted cells like metal wrap-through and interdigitated back-contact can be designed as bifacial cells [6-9].

Whether higher total irradiance levels can be translated into higher annual yield depends on the electrical and optical characteristics of the module. For bifacial modules a set of well-defined, widely adopted parameters that characterises the bifacial performance of a module is not yet available. Singh et al. proposed new characteristic STC parameters for bifacial cells based on measurement with illumination at front or rear with a dark back sheet [10]. At ECN a model is under development that aims to correlate data from STC measurements on bifacial modules to outdoor data. The outdoor performance of bifacial modules is measured for mini-modules and full-size modules. Irradiation of both planes of the module is measured separately, and orientation and albedo can be varied [11].

A model that correctly predicts the module performance using STC characteristics and outdoors irradiation and climate data is the basis of a reliable prediction of the annual energy production of PV systems with bifacial modules. Modelling of bifacial modules and systems is not yet as well-developed as for monofacial systems, for which well-tested and verified simulation tools like the PVSyst package [12] are available. In addition to changes in the electrical model required by simultaneous front and rear illumination, modifications are needed of the optical and thermal models for bifacial modules. Here, the outline of a comprehensive bifacial model is given. First validation results are presented as well as a comparison with a more simplified analysis using irradiance data only.

2. Bifacial model

A schematic of the bifacial model to calculate the DC output of a module is shown in Fig. 1. Only the meteorological data is the same as for monofacial modelling, all other parts are influenced by the bifacial irradiance and have to be adapted to that. The present model focusses on the DC output of the module, without effects of shading caused by the surroundings. Inverter specifications and system layout determine final AC energy yield.

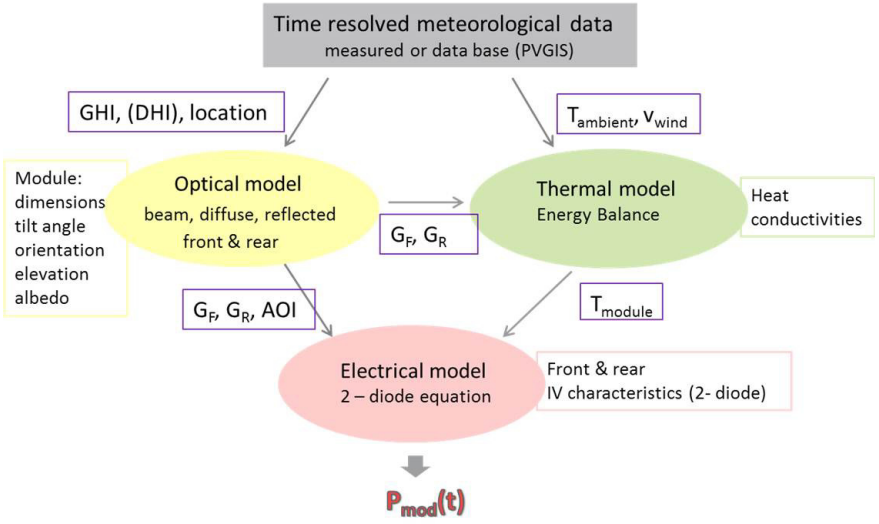

Fig.1 Schematic of the model to calculate the DC output of a bifacial module. Abbreviations and parameters are introduced in the text.

2.1 Optical model

The optical model requires data on the position of the sun and the total measured global horizontal irradiance (GHI) data at the location of the module. The diffuse horizontal irradiance G_d can be obtained from measured data or be derived from the GHI by applying a model e.g. the Erbs model [13]. The difference between the GHI and the G_d is the horizontal beam irradiation G_b. Following the anisotropic sky model a distinction is made between the circumsolar and isotropic diffuse irradiation, with the parameter A_i designating the fraction circumsolar irradiation. The resulting irradiance of beam, diffuse and ground-reflected light on a tilted module surface is calculated from the model in reference [13]. Specific for bifacial modules is that the ground reflection can be reduced by self-shading. This is incorporated by a view factor F_V, as described by Yusufoglu et al. [2]. It was assumed that this self-shading affects the reflection of both the beam and circumsolar diffuse light. Note that the approach described in [2] assumed the shading is uniform over the module. This is a simplification and has recently been modified Yusufoglu et al. [14]. This was not yet implemented in the presented model. The front irradiance G_F on a plane with tilt angle β and with a ground reflection (albedo) parameter γ is given by the sum of a) the direct and circumsolar diffuse irradiation, b) the isotropic diffuse irradiation, c) the ground reflected light due to isotropic diffuse irradiation and d) the ground reflected light due to direct and circumsolar diffuse irradiation:

$$G_F = (G_b + G_d A_i) R_{b,f} + G_d (1 - A_i) \left(\frac{1 + \cos\beta}{2}\right) f(\sin(\beta)) + G_d (1 - A_i) \gamma \left(\frac{1 - \cos\beta}{2}\right) + (G_b + G_d A_i) \gamma \left(\frac{1 - \cos\beta}{2} - F_{V,f}\right). \quad (1)$$

The factor $R_{b,f}$ is defined by

$$R_{b,f} = \frac{\cos\theta}{\cos\theta_s}, \quad (2)$$

with θ the angle of incidence (AOI in Fig. 1) and θ_s the sun's zenith angle. For a more detailed description of the various models we refer to the excellent textbook [13], including the $f(\sin(\beta))$. The irradiance at the rear G_R is described with a similar equation, where β and θ are replaced by their supplement and $F_{V,F}$ by the appropriate equivalent $F_{V,R}$. Notice, that the present implementation of the model ignores dependency of the reflection coefficient on the angle of incidence.

2.2 Thermal model

Due to the irradiation the module temperature T_{bif} will be higher than the ambient temperature T_{amb}. The thermal balance states that the power of front and rear irradiance corrected for the reflection and delivered electric power, equals the rate of heat conducted to the ambient. The heat conductivity is characterised by U_{bif}, the reflection coefficient is α_{bif} and the electrical output depends on the module efficiency η_{bif}:

$$U_{bif} \cdot (T_{bif} - T_{amb}) = \alpha_{bif} (G_F + G_R)(1 - \eta_{bif}). \quad (3a)$$

The equation adopted by PVSyst for a monofacial module implicitly assumes all radiation striking the rear of a free standing module is 100% reflected [12]:

$$U_{mono} \cdot (T_{mono} - T_{amb}) = \alpha_{mono} G_R (1 - \eta_{mono}). \quad (3b)$$

The values of the heat conductivity U_{bif} or U_{mono} depend on the mounting of the module and on the conductivity properties of the front glass and the rear glass or backsheet. Also the wind speed v must be taken into account for which usually a parametrisation $U_{module} = U_C + U_V v$ is used. Typical data from PVSyst for a free standing module are U_C = 25 $Wm^{-2}K^{-1}$, U_V = 1.2 $Wm^{-3}K^{-1}s$ and α_{mono} = 0.9 [12].

2.3 Electrical model

The electrical model uses a 2-diode approximation for both front and rear *IV* characteristics of the module, measured using a Pasan flash-tester in a reflection-free room. The *IV* curve for the total module output is obtained from parameters scaled with the front and rear irradiance. This approach was verified by simulations of a cell under simultaneous front and rear irradiance using the Atlas package [15]. Results will be presented in section 3.

The total current at short circuit $I_{T,SC}$ is written as:

$$I_{T,SC} = \frac{I_{F,SC}G_F + I_{R,SC}G_R}{G_{STC}}, \tag{4}$$

where $I_{F,sc}$ and $I_{R,sc}$ represent the I_{sc} as measured from, respectively the front and rear. The simulations showed that similar scaling can be applied for the diode parameters J_{01} and J_{02}, as well as the series resistance R_s. In most cases the relative difference for front or rear of these properties will be small but the operation of a cell as a rear junction or front junction cell will be reflected in these properties. Note, that the scaling of the J_0 value motivated the choice for the 2-diode model, as the J_{01} and J_{02} scaling seems more straightforward than scaling of the ideality factor n. So for $X = J_{01}, J_{02}, R_s$ the scaling is according to:

$$X = \frac{X_F G_F + X_R G_R}{G_F + G_R}. \tag{5}$$

2.4 Integrated model

The J_{01} and J_{02} values are corrected for the module temperature T using the method of PVSyst [12]:

$$J_{0n}(\mathrm{T}) = J_{0,ref}\left(\frac{T}{T_{ref}}\right)^3 \exp\left[\frac{qE_G}{nk}\left(\frac{1}{T_{ref}} - \frac{1}{T}\right)\right]. \tag{6}$$

This results in the final IV-curve for the module with front irradiation G_F and rear irradiation G_R:

$$I = I_{T,SC} - J_{0,1}(T)(\exp\left[\frac{(V+I\cdot R_S)q}{kT}\right] - 1) - J_{0,2}(T)(\exp\left[\frac{(V+I\cdot R_S)q}{2kT}\right] - 1) \tag{7}$$

Using this equation the maximum power output can be calculated.

2.5 Annual bifacial gain

The annual energy yield *AEY* is the summation of the calculated power output, using time resolved meteorological data. For verification and validation of the module the input is the actual measured meteorological data. For yield predictions meteorological data at a certain location can be synthetically generated from monthly average values in a data base such as PVGIS using PVSyst [1]. With a resolution in the data m_{year} points per year the annual energy yield is calculated by :

$$AEY(bif, DC) = \sum_{m\_year}(I_{MP}(i) * V_{MP}(i)). \tag{8}$$

The bifacial gain is then calculated as the ratio of the output of the bifacial module of interest over a south-oriented, optimum tilt angle, monofacial module in the same location:

$$\text{Bifacial gain} = \frac{AEY(bif,DC)}{AEY(mono,DC)} - 1. \tag{9}$$

3. Validation/Verification

3.1 Cell simulations

Fig. 2 shows the J_{SC}, as calculated in Atlas simulations, of an n-Pasha cell with simultaneous well-defined illumination from front and rear, a condition not so easily achieved under laboratory conditions. Here we present results for the case with the total front and rear irradiance equal to 1 Sun, and for the case where the front irradiance is fixed at 1 Sun and the rear contribution is varied from 0 to 1 Sun. The cell had a front side efficiency of 20.4% and a rear side efficiency of 19.5% corresponding with recently reported n-Pasha cell efficiencies [3]. In the simulation unit cell the metallisation fractions at front and rear were taken to be equal. The simulation results in Fig. 2a show that $J_{R,SC} < J_{F,SC}$, which is predominantly caused by the additional recombination at the illuminated side. This occurs at short–circuit conditions when the junction is at the opposite side of the wafer. This additional recombination is associated with the transport of minority carriers through the base. Fig. 2 also shows that the total J_{SC} is very well described by the scaling proposed in Eq. 4. The scaling is adequate for cases where the total irradiance is equal to one Sun, as well as cases where the total irradiance is up to two Suns.

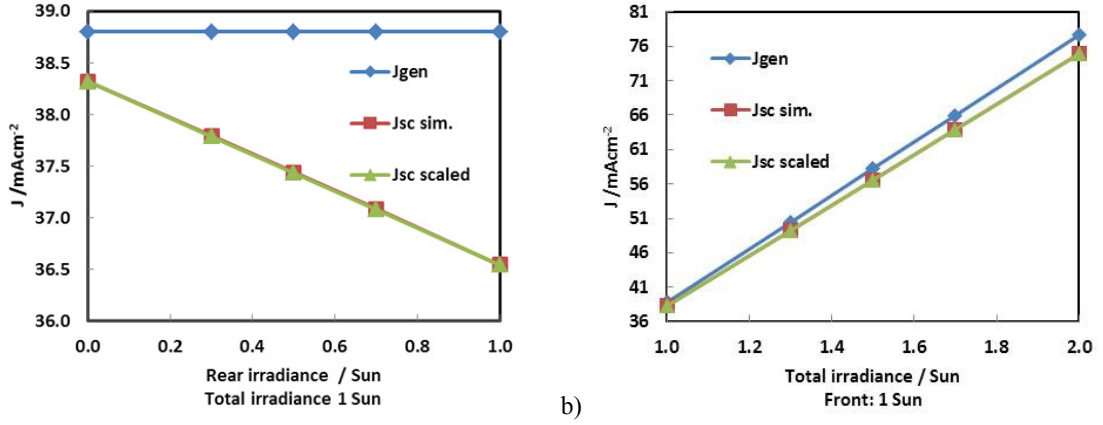

Fig. 2 The generated current density *Jgen* and the *Jsc* from cell simulations. Also shown is *Jsc* scaled obtained by applying eq. 4. a) the total irradiance is 1 Sun, b) the front irradiance is fixed at 1 Sun, with additional rear illumination.

Fig 3 shows simulated results for V_{OC}. At a total irradiance of 1 Sun the relative change in V_{OC} with varying front/rear ratio is only minor. But calculating J_{0F} and J_{0R} at, respectively, 1 Sun front and rear irradiance, from the V_{OC} and J_{SC} and then using Eq. 5 gives a better result than Eq. 4. At irradiance exceeding 1 Sun the dependence of V_{OC} on the total current is dominating and the scaling effect has a minor effect. Notice, that at high total irradiance the approximations overestimate the V_{OC}. The true V_{OC} in this case is limited by the increase of non-ideality that is associated with bulk recombination at high level injection.

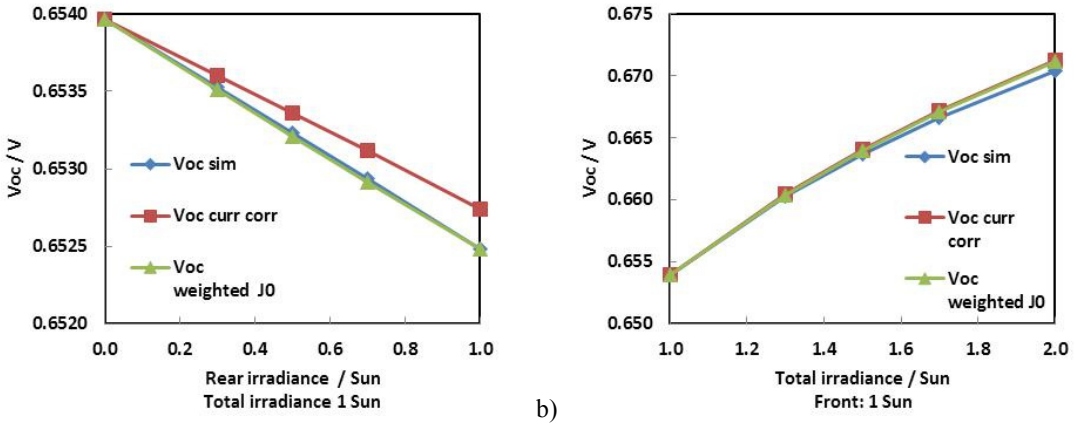

Fig. 3 The VOC as calculated in the simulations and approximations using a correction for the current only or with additionally J0 parameters weighted according to eq. 5. a) and b) as in Fig. 2

Like the V_{OC}, the fill factor *FF* shows little variation as long as the total irradiance is at 1 Sun. As a result the efficiency (measured with respect to the total irradiance) is an irradiance weighted average of the front and rear efficiency.

In the case the total irradiance is larger than one Sun, the V_{OC} will increase but the associated increase in efficiency is partly cancelled due to higher resistive losses that reduce the *FF*. In the present simulations this still results in a slightly higher efficiency than would be expected on the basis of scaling according to Eq. 5, as shown in Fig. 4a. Note, that in this simulation only resistive losses in the wafer are included. Conversely, at very low irradiance the efficiency is limited by decrease in V_{OC} as Fig. 4b shows. Of course these results depend strongly on the actual parametrisation used but we think this parametrisation reflects well the properties of the n-Pasha cell [3]. The observed deviations from scaled efficiency indicate that both cases of low and high total irradiance require the more complete treatment of the electrical behaviour given by Eq. 7.

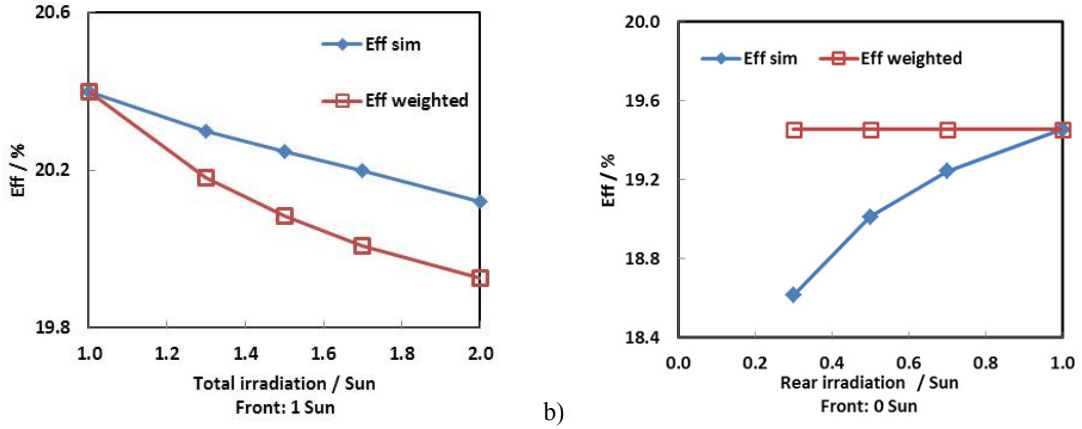

Fig. 4 The efficiency as calculated in the simulations and weighted according to eq. 5. a) the front irradiance is 1 Sun, with additional rear illumination and b) the front irradiance is zero with rear irradiance up to 1 Sun.

The simulation shows that efficiency difference under front or rear illumination is mainly caused by the I_{SC}. This is in agreement with the observation that for modules the ratio $I_{R,SC}/I_{F,SC}$ is almost identical to the ratio of the nominal maximum power output under rear and front illumination, the bifaciality factor. In general, the origin of the difference in I_{SC} is in differences in the metallisation fraction at front and rear, the presence of a front or rear

junction, the antireflection coatings, the surface recombination and the free-carrier absorption. These differences are to some extent unavoidable due to the different polarity at front and rear. On the other hand they can be minimised by tailoring these properties to the need of bifacial applications rather than monofacial applications.

3.2 Outdoor measurements

Fig. 5a shows one example of outdoor observations made at the set-up described in [11]. A 2x2 n-type Si cell laminate was placed vertically, with the front facing either East or West. The ground surface was either concrete or covered with a white sheet to mimic light-reflecting paint. Data was taken at regular intervals whilst changing orientation (front/rear) and ground cover, thereby changing the angle of incidence and the irradiance. The bifaciality factor of this laminate is about 93%. The increased power output with a white ground cover is the same for front and rear with a gain of about 19%, compared to about 5% on light-grey concrete.

We also logged the irradiance on the rear G_R, using a calibrated reference cell. Combining STC measurements of the front and the rear and the logged G_F and G_R, we calculated $I_{T,SC}$, according to Eq. 4. For each observation, the observed I_{SC} is plotted against the calculated $I_{T,SC}$ in Fig. 5b. This graph covers a wide range of I_{SC} values and conditions, since measurements were done both under "blue sky" conditions and on a day with large variation in cloud coverage.

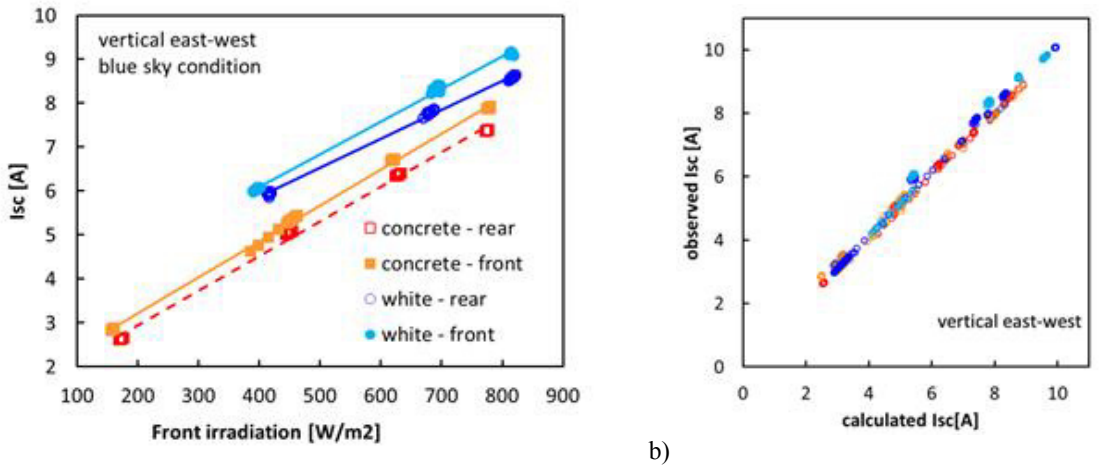

Fig. 5 a) Observed Isc as a function of GF with two types of ground surface (albedo) under blue sky conditions. b) Observed Isc as a function of the calculated Isc, according to eq.4, the legend is valid for both graphs.

4. Predicted annual bifacial gain

4.1 Predicted irradiance

Fig. 6 shows the calculated yearly irradiance on bifacial, vertically mounted east-west oriented modules elevated 0.5 m above the ground, and monofacial south oriented modules with optimum tilt angle using synthetic hourly data generated from PVGIS Climate-SAF monthly values [16] for Amsterdam and Doha. The total irradiance on the front and rear of a vertical east-west module can easily equal or exceed the irradiation on a south facing monofacial module, and this difference increases significantly with higher albedo values. In both locations a major source of irradiance gain of the bifacial systems is from the ground reflection. The total irradiance gain for bifacial modules will therefore increase strongly with the albedo. The total direct and circumsolar irradiance on the bifacial module is in both locations smaller than on the monofacial one. The reverse holds for the isotropic diffuse light. In Amsterdam the total of beam, circumsolar and isotropic light hitting each type of module is fairly similar. This means a small

albedo is already sufficient to cause a gain in total irradiance. In Doha a larger albedo is required. Note that for these vertical modules the self-shading effect is not very pronounced and therefore the crude approximation, as explained in section 2.3, made when calculating $F_{V,F}$ and $F_{V,R}$ will not seriously impact the results.

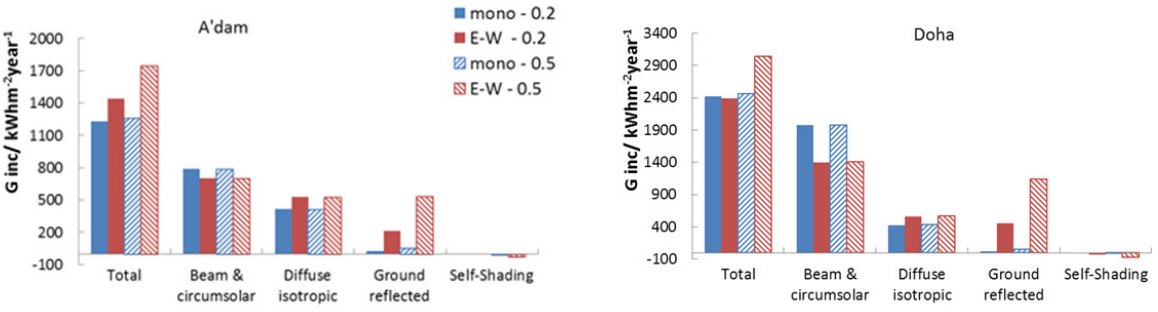

a) b)

Fig. 6 a) Calculated irradiance in a) Amsterdam and b) Doha on a monofacial south-facing module with optimum tilt angle and a vertical east-west module. The numbers in the legend, valid for both graphs, indicate the albedo value used in the calculations.

4.2 Predicted energy output

Whether higher total irradiance levels can be translated into higher annual yield depends on the module front and rear characteristics. A 72 cell module of n-Pasha cells at ECN showed an STC front and rear encapsulated cell efficiency of 18.2 % and 16.8 % respectively [17]. With a reflecting backsheet the monofacial efficiency would be 18.7%. A first guess of bifacial gains can be made by scaling the rear irradiance with the bifacial factor, i.e. in this case 92.3 %, and using the STC front efficiency. The annual power output of the bifacial module is then calculated from:

$$AEY(bif, scaled) = \sum_{m\_year} \left(G_{T,front}(i) + f_b G_{T,rear}(i) \right) \eta_{front}(i) \qquad (10)$$

The yield of the monofacial module is calculated similarly using only front irradiance and the STC efficiency of the monofacial module, and the bifacial gain is derived from Eq. 9. The calculated gains are shown in Table I. These data predict that with a good bifaciality factor in locations like Amsterdam substantial gains can be expected, and in Doha as well if the albedo is large.

Table 1. Calculated bifacial gain of bifacial E-W modules with respect to monofacial south oriented modules

Location- albedo	A'dam-0.2	A'dam-0.5	Doha-0.2	Doha-0.5
Scaled irradiance	9.2%	29.0%	-7.8%	15.3%
Electrical model,25°C	10.1%	30.6%	-9.4%	14.8%
Full model	10.4%	29.5%	-5.6%	17.2%

The bifacial gain was also calculated using the electric model, Eq. 4-7, but fixing the temperature at 25°C, and with the full model, i.e. also the thermal corrections from Eq. 3. In this equation the parameters quoted in section 2.2 were used together with a fixed module efficiency of 16%, a value consistent with high irradiance conditions. The bifacial gains calculated here with the full model are slightly larger than obtained with the scaled irradiance model.

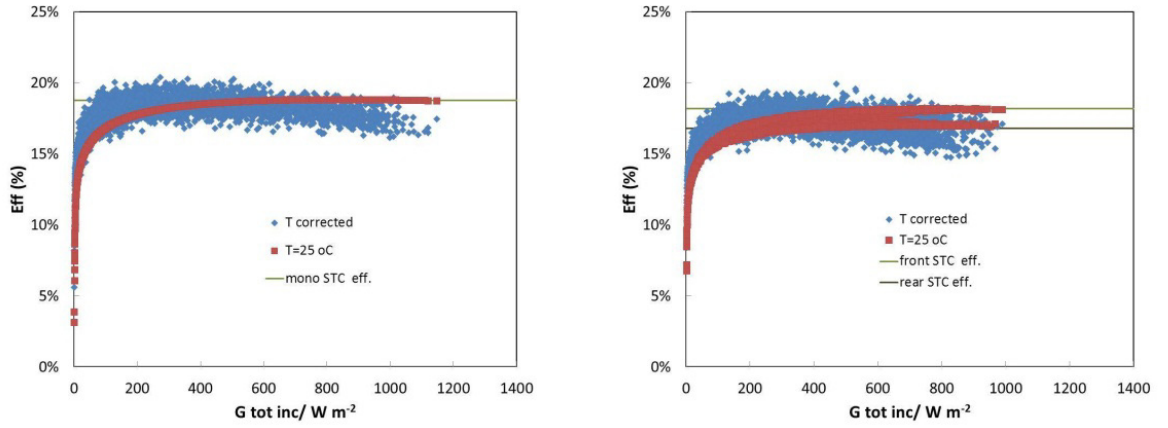

Fig. 7 Efficiency as a function of irradiance on a) a monofacial south oriented module in Amsterdam albedo 0.2 and b) an east-west facing module vertical bifacial module at the same location and albedo. The temperature correction was done using meteorological data for a whole year.

Fig. 7 shows the distribution of the calculated efficiency as a function of the total irradiance for the location in Amsterdam with albedo 0.2. When the electrical model is applied, the reduction of the V_{OC} causes a lower efficiency at low incident radiation. At high incident radiation the increase in efficiency levels off, as the V_{OC} effect is compensated by the resistive effect. The compensation by resistive losses seems stronger for the monofacial module than for the bifacial module. The increase in bifacial gain calculated for Amsterdam with the electrical model seems therefore due to reduced resistive losses in the bifacial module. Fig. 7 shows that at high irradiance level the efficiency is reduced because of the temperature of the module. In a location like Amsterdam the temperature has minor effect on the gain, but in Doha, with on average much higher irradiance and ambient temperature, the corrections may be significant.

The bifacial gains of 10% to 30% are in line with the observations on energy yield gains reported in e.g. [11], Note, that the bifacial gain presented here is a DC gain. The AC gain may be differ from this because of additional inverter and system aspects. Moreover, the non-uniformity of the current in the module due to non-uniform self-shading was ignored. This may reduce the bifacial gain.

5. Conclusions

Accurate modelling is required to quantify the gain that may be expected from increased irradiance on bifacial modules. We presented a model with optical, electrical and thermal aspects tailored to bifacial modules.

As a first validation step, we showed that the front and rear I_{sc} can be added, when weighted with the front and rear irradiance. This gives already a good approximation to the expected efficiency under bifacial operations. The model can be further extended by scaling other parameters of the 2-diode front and rear *IV*-curves. Finally, our results show that the relative AEY gain of bifacial east-west modules over south-oriented monofacial modules increases strongly with albedo. In a location like Amsterdam the gain is 10% at albedo 0.2 and 30% at albedo 0.5. Although the module temperature has a large effect on the annual energy yield, the bifacial gain will be less effected.

Further extensions of this model, including the effect of shading by surroundings, the inverter and system aspects similar to those required for standard monofacial systems, are needed to obtain realistic AC annual energy yields.

Acknowledgements

This work was partially funded by the Dutch TKI Solar Energy project NChanted. http://www.tkisolarenergy.nl/

References

[1] S. Guo, T. M. Walsh, and M. Peters, Vertically mounted bifacial photovoltaic modules: A global analysis, Energy, **61**, 447-454 (2013).
[2] U. A. Yusufoglu, T. H. Lee, T. M. Pletzer, A. Halm, L. J. Koduvelikulathu, C. Comparotto, R. Kopecek, and H. Kurz, Simulation of Energy Production by Bifacial Modules with Revision of Ground Reflection, Energy Procedia, **55**, 389-395 (2014).
[3] G. J. M. Janssen, M. Koppes, Y. Komatsu, J. Anker, J. Liu, A. Gutjahr, A. A. Mewe, C. J. J. Tool, I. G. Romijn, O. Siarheyeva, M. A. Ernst, B. H. W. van de Loo, and W. M. M. Kessels, Front side improvements for n-Pasha solar cells, 29th European Photovoltaic Solar Energy Conference, Amsterdam (2014).
[4] J. Libal, V.D. Mihailetchi and R. Kopecek, Low-cost, high-efficiency solar cells for the future: ISC Konstanz's technology zoo, Photovoltaics International, **23**, 35-45 (2014).
[5] F. Fertig, K. Krauss, J. Greulich, F. Clement, D. Biro, R. Preu, and S. Rein, The BOSCO Solar Cell: Double-sided Collection and Bifacial Operation, Energy Procedia, **55**, 416-424 (2014).
[6] N. Guillevin, L. J. Geerligs, L. Okel, B. B. van Aken, I. J. Bennett, A. Gutjahr, J. Wang, Z. Wang, J. Zhai, Z. Wan, S. Tian, Z. Hu, G. Li, B. Yu, and J. Xiong, High Efficiency n-Type Metal-Wrap-Through Cells and Modules Using Industrial Processes, 29th European Photovoltaic Solar Energy Conference, Amsterdam (2014).
[7] T. Mishima, M. Taguchi, H. Sakata, and E. Maruyama, Development status of high-efficiency HIT solar cells, Solar Energy Materials and Solar Cells, **95**, 18-21 (2011).
[8] I. Cesar, N. Guillevin, A. R. Burgers, A. A. Mewe, M. Koppes, J. Anker, L. J. Geerligs, and A. W. Weeber, Mercury: A Back Junction Back Contact Front Floating Emitter Cell with Novel Design for High Efficiency and Simplified Processing, Energy Procedia, **55**, 633-642 (2014).
[9] V. Mihailetchi, Zebra, bifacial IBC technology, 2nd Bifacial Workshop Chambery (2014).
[10] J. P. Singh, T. M. Walsh, and A. G. Aberle, A new method to characterize bifacial solar cells, Prog.Photovolt: Res.Appl., **22**, 903-909 (2014).
[11] B. B. van Aken, M. J. Jansen, A. J. Carr, G. J. M. Janssen, and A. A. Mewe, Relation between Indoor Flash Testing and Outdoor Performance of Bifacial Modules, 29th European Photovoltaic Solar Energy Conference, Amsterdam (2014).
[12] PVsyst V6, Premium, Photovoltaic System Software, 2013, www.pvsyst.com. Last accessed May 2015.
[13] J. A. Duffie and W. A. Beckmann, Solar Engineering of Thermal processes, 2nd ed., John Wiley &Sons, 1991.
[14] U. A. Yusufoglu, T. Lee, T. Pletzer, H. Kurz, A. Halm, L. J. Koduvelikulathu, C. Comparotto, and R. Kopecek, Modeling and simulation of annual energy yields of bifacial modules at different climate zones, 2nd Bifacial Workshop Chambery (2014).
[15] Atlas, Atlas, 2013, www.silvaco.com.
[16] PVGIS, 2013, http://re.jrc.ec.europa.eu/pvgis/apps4/pvest.php#. Last accessed May 2015.
[17] I. G. Romijn, B. B. van Aken, J. Anker, A. R. Burgers, A. Gutjahr, B. Heurtault, M. Koppes, E. Kossen, M. Lamers, D. S. Saynova, L. Fang, X. Jingfeng, X. Zhuo, and A. H. G. Vlooswijk, Industrial Implementation of Efficiency Improvements in n-Type Solar Cells and Modules, 27th European Photovoltaic Solar Energy Conference; Frankfurt, Germany; Munich, WIP-Renewable Energies; 533-537 (2012).